

Sialic Acid–Siglec-E Interactions Regulate the Response of Neonatal Macrophages to Group B *Streptococcus*

Sean J. Lund,* Pamela G. B. Del Rosario,*[†] Asami Honda,* Kaitlin J. Caoili,[‡] Marten A. Hoeksema,[§] Victor Nizet,* Kathryn A. Patras,[¶] and Lawrence S. Prince[‡]

*Department of Pediatrics, University of California, San Diego, La Jolla, CA; [†]Rady Children's Hospital, San Diego, CA; [‡]Department of Pediatrics, Stanford University, Palo Alto, CA; [§]Department of Medical Biochemistry, Amsterdam University Medical Center, Amsterdam Zuidoost, the Netherlands; and [¶]Department of Molecular Virology and Microbiology, Alkek Center for Metagenomics and Microbiome Research, Baylor College of Medicine, Houston, TX

ABSTRACT

The mammalian Siglec receptor sialoadhesin (Siglec1, CD169) confers innate immunity against the encapsulated pathogen group B *Streptococcus* (GBS). Newborn lung macrophages have lower expression levels of sialoadhesin at birth compared with the postnatal period, increasing their susceptibility to GBS infection. In this study, we investigate the mechanisms regulating sialoadhesin expression in the newborn mouse lung. In both neonatal and adult mice, GBS lung infection reduced *Siglec1* expression, potentially delaying acquisition of immunity in neonates. Suppression of *Siglec1* expression required interactions between sialic acid on the GBS capsule and the inhibitory host receptor Siglec-E. The *Siglec1* gene contains multiple STAT binding motifs, which could regulate expression of sialoadhesin downstream of innate immune signals. Although GBS infection reduced STAT1 expression in the lungs of wild-type newborn mice, we observed increased numbers of STAT1⁺ cells in *Siglec1*^{−/−} lungs. To test if innate immune activation could increase sialoadhesin at birth, we first demonstrated that treatment of neonatal lung macrophages ex vivo with inflammatory activators increased sialoadhesin expression. However, overcoming the low sialoadhesin expression at birth using in vivo prenatal exposures or treatments with inflammatory stimuli were not successful. The suppression of sialoadhesin expression by GBS–Siglec-E engagement may therefore contribute to disease pathogenesis in newborns and represent a challenging but potentially appealing therapeutic opportunity to augment immunity at birth. *ImmunoHorizons*, 2024, 8: 384–396.

INTRODUCTION

Group B *Streptococcus* (GBS; *Streptococcus agalactiae*) remains a leading neonatal pathogen (1). A frequent colonizer of the maternal birth canal, GBS causes ascending infections of newborn infants around the time of delivery. GBS infection can present with acute and sometimes fulminant pneumonia and sepsis or, alternatively, a more indolent later-onset bacteremia and meningitis (2). For incompletely understood reasons, serious GBS

infections occur primarily in newborns, then remain quite rare in older infants, children, and healthy adults, with the exception of the elderly or those with chronic illness or immunosuppression (3). The unique susceptibility of newborns to GBS infection suggests novel host–pathogen interactions between the developing newborn immune system and specific bacterial virulence factors.

Airway epithelial cells and resident immune cells protect the lung against microbial pathogens (4). Alveolar macrophages

Received for publication September 13, 2023. Accepted for publication April 24, 2024.

Address correspondence and reprint request to: Dr. Lawrence S. Prince, Stanford University School of Medicine, Lucile Packard Children's Hospital Stanford, Center for Academic Medicine – 434B, Division of Neonatology – MC: 5660, 453 Quarry Road, Palo Alto, CA 94304. E-mail address: lsprince@stanford.edu
ORCIDs: 0000-0001-5028-4388 (A.H.); 0000-0003-3847-0422 (V.N.); 0000-0003-2631-8810 (K.A.P.); 0000-0002-7010-4548 (L.S.P.).

This work was supported by National Institutes of Health Grants HL146066 (to S.J.L.), AI142864 (to L.S.P. and V.N.), HL126703 (to L.S.P.), and HL107150 (to V.N.). K.A.P. was supported by a University of California Chancellor's Postdoctoral Fellowship and Hartwell Foundation Fellowship. M.A.H. was supported by an American Heart Association Fellowship.

Abbreviations used in this article: ATAC-seq, assay for transposase-accessible chromatin with sequencing; BMDM, bone marrow–derived macrophage; ChIP-seq, chromatin immunoprecipitation sequencing; GBS, group B *Streptococcus*; OCR, open chromatin region; PND, postnatal day; PPAR γ , peroxisome proliferator-activated receptor γ ; WT, wild type.

This article is distributed under the terms of the [CC BY-NC 4.0 Unported license](https://creativecommons.org/licenses/by-nc/4.0/).

Copyright © 2024 The Authors

are the primary immune cell within the lung, initially detecting inhaled microbes and particles (5). For pathogen detection, alveolar macrophages express a variety of pattern recognition receptors that activate innate immune signaling pathways. Sialic acid-binding Ig-like lectins, or Siglecs, are a family of important cell surface membrane receptors on alveolar macrophages, mediating the detection of glycan molecules present on many microbial species (6). Interactions between the heavily sialylated GBS capsule and immune cell Siglecs can drive both bacterial killing and immune tolerance. The alveolar macrophage marker Siglec-F (also known as Siglec5 and encoded by the *Siglecf* gene) increases in the days following birth (7). Sialoadhesin, a specific well-conserved mammalian Siglec receptor, coordinates innate and adaptive immune defenses against GBS and other sialylated bacterial pathogens (8). In contrast, human Siglec-9 and its murine homolog Siglec-E inhibit the innate immune response upon binding similar glycan structures (9–11).

We previously demonstrated that the developmental regulation of lung macrophage Siglec expression provides a window of opportunity for persistent, severe GBS infection in newborn mice (12). Although the inhibitory Siglec-E was expressed on lung macrophages at all developmental time points, sialoadhesin expression was low in newborns, increasing in the days following birth. With macrophages expressing a protolerance immune receptor (Siglec-E) without the receptor required for bacterial killing (sialoadhesin), GBS uses its sialic acid capsule to evade a robust innate immune response in newborn lungs. These studies suggested influencing the developmental regulation of sialoadhesin expression, and bacterial glycan detection in newborns could represent a new therapeutic approach to prevent serious infections.

Although sialoadhesin expression normally increases in the days following delivery, more rapid elevation of expression levels right at birth might be protective against neonatal GBS infection. Alternatively, regulating GBS-mediated immune suppression could prove equally advantageous. In this study, we explore molecular mechanisms that regulate sialoadhesin expression in the newborn mouse lung. By using both in vivo and ex vivo experimental models, we tested the host–pathogen interaction mechanisms linked to Siglec expression and the ability of specific mediators to influence receptor expression. These data provide an important basis for therapeutic strategy development and understanding of the basic mechanisms of newborn immunity.

MATERIALS AND METHODS

Mice

All animal experiments were approved the University of California, San Diego, and Stanford University institutional animal care and use committees. Wild-type (WT) (C57BL/6) mice were obtained from Envigo. *Stat6*^{−/−} mice were provided by Dr. Taylor Doherty, and *Siglece*^{−/−} mice (9) (The Jackson Laboratory, strain 032008) were provided by Dr. Ajit Varki.

Bacteria

The GBS strain COH1 (American Type Culture Collection, BAA-1176), a highly encapsulated serotype III neonatal meningitis isolate with established virulence in rodent models of pneumonia, sepsis, and meningitis, was used for murine infections. GBS was propagated in Todd-Hewitt broth. We also used the Δ *neuA* GBS mutant generated previously (13), which carries an isogenic, in-frame allelic replacement mutation in the *neuA* gene and lacks the terminal sialic acid of the capsule side chain (14).

Pneumonia model

To prepare bacteria for inoculation, an overnight culture of GBS in Todd-Hewitt broth was subcultured and grown to mid-logarithmic phase ($OD_{600} = 0.4$). One milliliter of the subcultured GBS was collected by centrifugation, washed with HBSS, and resuspended in HBSS for inoculation. Adult and neonatal mice, under light anesthesia with 3% isoflurane and spontaneously breathing, were infected with 28,000 CFU/g body weight COH1 GBS via intranasal administration. Adult inoculations were administered in 50 μ l, whereas neonatal mice received 2 μ l. Animals were monitored until they recovered from anesthesia. Survival was monitored for 21 d, and any animal showing signs of severe disease was humanely euthanized.

Intraperitoneal injections

Timed pregnant dams were i.p. injected with either a vehicle control, IFN α (2.5 μ g), IFN γ (1 μ g), or rosiglitazone (0.1 mg or 0.5 mg). The treated dams were closely monitored for signs of distress twice daily following injection for a total of 1 wk following injection. After delivery, the neonates were also observed for signs of distress or poor nursing.

Ex vivo cell culture and treatment

To test potential therapeutic agents ex vivo, postnatal day 2 (PND2) neonatal lungs were digested into single-cell suspensions. Cells were plated at a density of 10^6 cells/well in a 12-well plate and subsequently treated for 8, 14, or 38 h with LPS (250 ng/ml), Pam₃CSK₄ (300 ng/ml), GM-CSF (10 ng/ml), TNF α (10 ng/ml), or IFN γ (10 ng/ml). Following treatment, the cells were removed from culture and analyzed by flow cytometry.

Flow cytometry

Following euthanasia and lung perfusion with PBS, the left lobes of both adult and neonatal mice were digested in RPMI containing 2 mg/ml of collagenase IV for 15 min. The resulting single-cell suspension was passed through a 70- μ m filter and collected by centrifugation. Cells were stained with the following Abs: CD45 (BD Biosciences), CD11b (BioLegend), CD11c (BioLegend), CD64 (BioLegend), F4/80 (BioLegend), Siglec-F (BD Biosciences), Gr-1 (BioLegend), MHC-II (BioLegend), Siglec-E (BioLegend), and CD169/sialoadhesin (BioLegend) for 30 min at 4°C. After staining, the cells were washed,

resuspended in FACS buffer, and studied using a BD FACS-Canto II. Data were analyzed using FlowJo software.

RNA extraction and cDNA synthesis

The cranial and accessory lobes of both adult and neonatal lungs were snap frozen using ethanol and dry ice. For RNA extraction, the lungs were homogenized in TRIzol. Isolated RNA was then resuspended in molecular grade water for quantification using a NanoDrop spectrophotometer. cDNA synthesis was performed using a Superscript III Reverse Transcription Kit (Invitrogen) according to the manufacturer's protocol.

Real-time PCR

Real-time PCRs were performed using a Bio-Rad CFX96 Touch Real-time System with gene-specific primers (IDT) and SYBR Green (Bio-Rad Laboratories) detection. Each sample was measured in triplicate, and ΔC_T values were calculated using *Gapdh* as a control transcript for normalization. For comparison of gene expression between samples and conditions, control samples were obtained from uninfected animals, and changes in expression were plotted using the $2^{-\Delta\Delta C_T}$ method. Each sample replicate is presented in the graphs.

Transcription factor prediction and analysis of assay for transposase-accessible chromatin with sequencing (ATAC-seq) and chromatin immunoprecipitation sequencing (ChIP-seq) data

To explore the genetic regulation and enhancer networks of *Siglec1* and *Siglec*, we used three different online databases: the Immunological Genome Project (ImmGen) data browser Enhancer Networks, ChIPBase version 2.0, and ConTra version 3. Using ImmGen data browser Enhancer Networks, we searched for *Siglec1* and *Siglec* enhancer networks. ImmGen provided open chromatin regions (OCRs) within the gene locus, color-coded on the basis of the strength of correlation between activity and expression. This approach identified the transcription factors most likely to control these OCRs. A ChIPBase Network search was also performed for both *Siglec1* and *Siglec*. This database searches for transcription factor binding sites within 1 kb upstream and downstream of the transcription start site, reporting the total number of transcription factor binding sites. ConTra version 3 is similar to ChIPBase but allows manual searching of specific transcription factors and provides a visualization of binding sites in both the promoter and gene regions. Previously published ATAC-seq (15) and ChIP-seq data (16, 17) were visualized using the UCSC Genome Browser to compare OCRs and STAT binding frequencies in and around the murine *Siglec1* and *Siglec* genes.

Immunofluorescence and confocal microscopy

The left lobes of both adult and neonatal mice were removed and fixed in 4% paraformaldehyde for 1 h at room temperature. Following fixation, the lungs were washed in PBS containing

Ca and Mg, processed through sucrose gradients, and frozen in optimal cutting temperature compound for sectioning by the UC San Diego Moores Cancer Center Histology Core. Each frozen slide was briefly fixed in 2% paraformaldehyde for 20 min, permeabilized with 0.1% Triton X-100 for 5 min, and blocked with 5% donkey serum and 5% goat serum for 1 h at room temperature. Slides were incubated with primary Abs (anti-CD68, OriGene; anti-STAT1, Thermo Fisher) in 1% BSA and 0.1% Triton X-100 overnight. Secondary anti-rat Alexa Fluor 488 and anti-rabbit Alexa Fluor 555 were used for detection along with DRAQ5 (1 μ m, Thermo Fisher) for staining of nuclei. Slides were mounted in ProLong Gold (Life Technologies) and cured overnight. Images were obtained using a Leica TCS-SPE laser scanning confocal microscope. Z-stack image sets were obtained using a 40 \times objective. Images were exported in Leica LAS-X software, and resolution and size were set in Affinity Photo for inclusion in figures. For quantification of anti-STAT1 fluorescence, images were imported into ImageJ. Total fluorescence in the STAT1 channel was measured for each image and divided by the total nuclear fluorescence in the DRAQ5 channel to normalize for cell number.

Statistics

Statistical analyses were performed using GraphPad Prism. Data were primarily compared using the nonparametric Mann-Whitney *U* test. For experiments depicting the fold change in mRNA expression as measured by real-time PCR, the parametric two-tailed unpaired *t* test was used, comparing the ΔC_T values (between the gene of interest and the housekeeping gene *Gapdh*). In the figures, *p* values <0.05 are considered statistically significant and denoted with a single asterisk. *p* values <0.01 are denoted with two asterisks, *p* values <0.005 are denoted with three asterisks, and *p* values <0.001 are denoted with four asterisks.

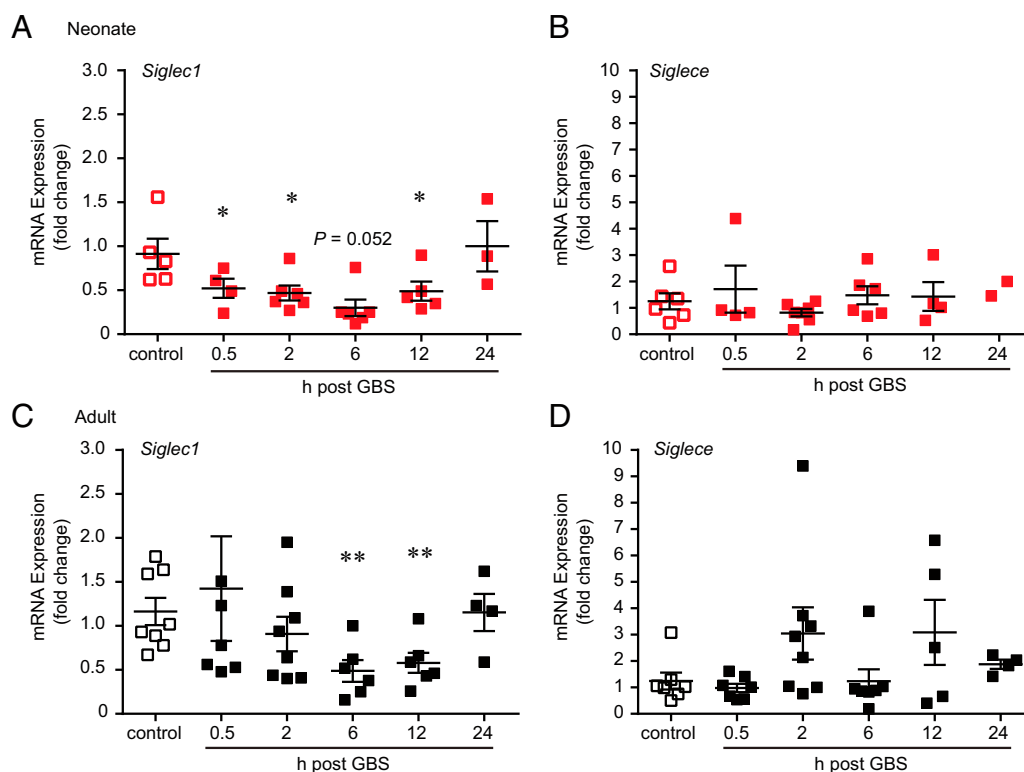
RESULTS

GBS inhibits sialoadhesin expression in infected lungs

Low levels of sialoadhesin expression at birth render newborn mice susceptible to GBS pneumonia (12). However, sialoadhesin expression increases during the postnatal period, providing protection. The mechanisms by which GBS exposure regulates Siglec receptor expression remain unclear. Using a newborn mouse GBS pneumonia model, we collected whole-lung RNA in a longitudinal time course within the first 24 h following GBS infection. Control mice received sterile HBSS instillation. Adult mice were also infected with GBS for comparison. In both neonatal and adult mice, GBS infection coincided with reduced *Siglec1* mRNA expression (which encodes sialoadhesin) within hours postinfection (Fig. 1). Inhibition appeared transient because *Siglec1* mRNA levels returned to baseline by 24 h postinfection in both neonates and adults. By contrast, the expression of *Siglec* mRNA (which encodes Siglec-E/CD170, a receptor that binds identical glycan structures as sialoadhesin

FIGURE 1. GBS infection reduces *Siglec1* expression.

Neonatal (A and B) or adult (C and D) C57BL/6 mice were infected with GBS, and whole-lung RNA was isolated 0.5, 2, 6, 12, or 24 h following infection. Expression of *Siglec1* (the gene encoding sialoadhesin; A and C) and *Siglece* (encoding Siglec-E; B and D) was measured by real-time PCR and compared with *Gapdh* expression. Values were normalized to control, uninfected RNA samples and plotted using the $2^{-\Delta\Delta CT}$ calculation. * $p < 0.05$, ** $p < 0.01$ using an unpaired, two-tailed t test. Each data point represents an individual infected or uninfected mouse.



but inhibits inflammatory signaling) remained unchanged upon GBS infection. These findings suggested that GBS infection suppresses the expression of a key host glycan receptor essential for immune protection.

We hypothesized that engagement of the GBS capsular glycans with the inhibitory receptor Siglec-E reduces *Siglec1* expression. To test this hypothesis, we infected neonatal WT and *Siglece*^{-/-} mice with GBS and measured sialoadhesin expression in alveolar macrophages by flow cytometry. Consistent with the mRNA expression data, GBS infection resulted in a decrease in sialoadhesin expression on the surface of neonatal alveolar macrophages (Fig. 2A). However, in *Siglece*^{-/-} mice, GBS had no effect on sialoadhesin expression. In control neonatal mice, Siglec-E was undetected in a subpopulation of lung macrophages. Following GBS infection, Siglec-E protein expression was increased on the cell surface of WT macrophages, suggesting it potentially contributes to additional suppression of the immune response and reduced bacterial killing.

Because both sialoadhesin and Siglec-E recognize glycans with terminal sialic acids, we next tested the requirement of GBS sialic acid for inhibiting *Siglec1* expression by using the Δ neuA GBS strain, which lacks a functional NeuA enzyme critical for incorporating sialic acid into the polysaccharide capsule (14). Infection of both neonatal and adult mice with Δ neuA GBS did not result in the same inhibition of *Siglec1* expression seen with WT GBS (Fig. 2B, 2C). These results indicated that GBS sialic acid is necessary for suppressing *Siglec1* expression.

The inflammatory response to Δ neuA GBS was also impacted. In newborn mice infected with WT GBS, *Il1b* expression

increased 24 h postinfection (Fig. 2D). However, Δ neuA GBS infection did not induce the same increase in cytokine expression. In contrast, in adult mice, Δ neuA GBS infection stimulated a robust increase in *Il1b* after 6 h, suggesting that adult lungs possess additional innate immune response mechanisms that are independent of bacterial sialic acid recognition. Collectively, these data emphasized the importance of Siglecs and the recognition of bacterial sialic acid motifs in suppressing receptor-mediated immune activation following GBS infection.

Potential interactions between Siglecs and STAT signaling

To better understand the potential molecular mechanisms regulating sialoadhesin expression during GBS infection, we first examined promoter and enhancer regions within the murine *Siglec1* and *Siglece* genes (Fig. 3A–3C). Using ChIPBase version 2.0, ImmGen Enhancer Networks, and ConTra version 3, we identified predicted binding sites for STAT1 and STAT6 in the *Siglec1* gene, consistent with prior studies (18–23). The low sialoadhesin expression in newborn macrophages could be due to developmental differences in promoter and enhancer accessibility. We therefore examined ATAC-seq and ChIP-seq datasets (Fig. 3D, 3E) generated from neonatal and adult alveolar macrophages after in vivo LPS treatment and bone marrow-derived macrophages (BMDMs) treated in vitro with either IL-4 (to examine STAT6 binding) or IFN γ (to examine STAT1 binding) (15–17).

Although ATAC-seq and ChIP-seq peaks at the *Siglec1* promoter were similar across samples, distant regions upstream and downstream of the *Siglec1* gene contained more open

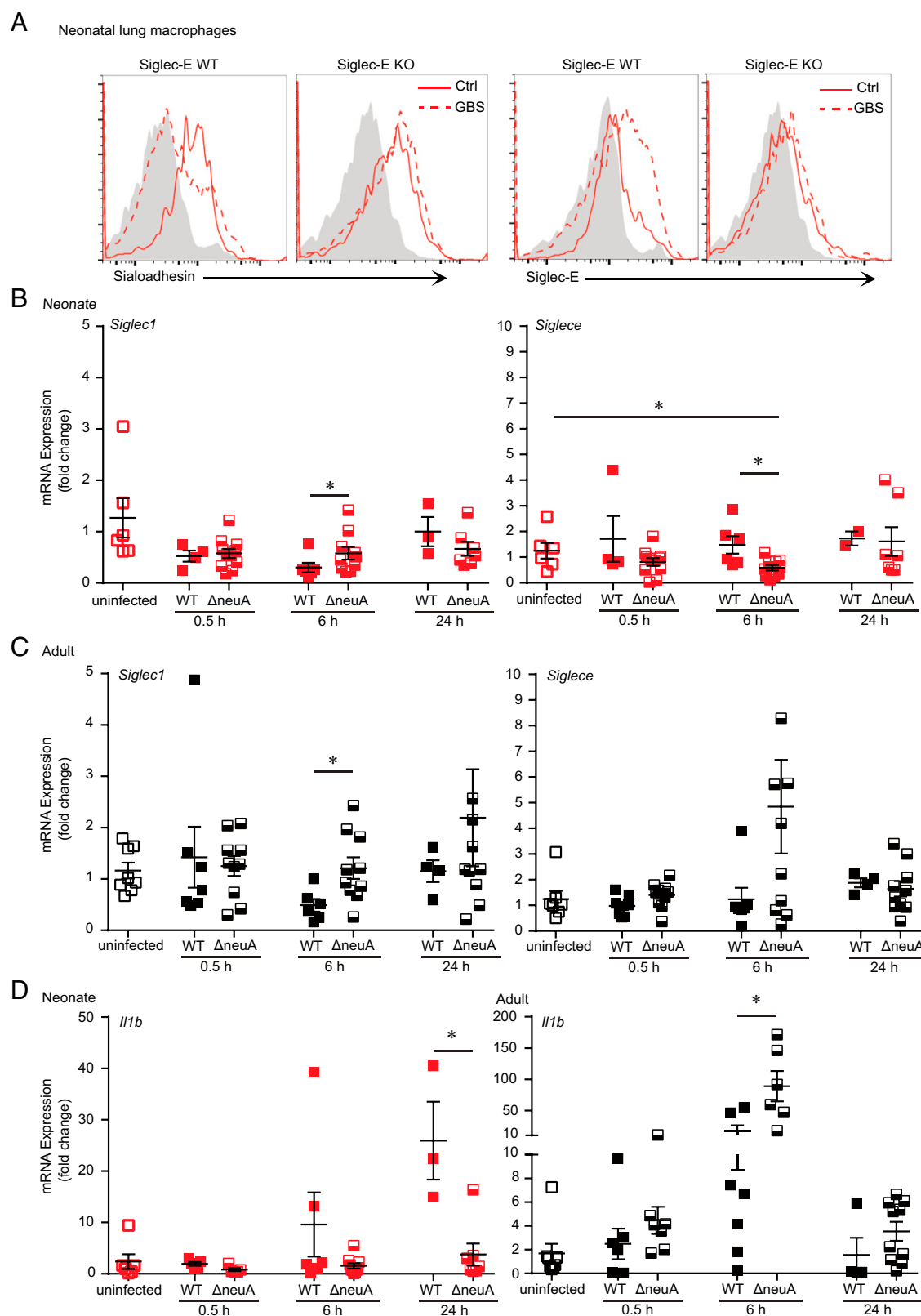


FIGURE 2. Inhibition of sialoadhesin expression following GBS infection requires Siglec-E and GBS capsular sialic acid.

(A) Neonatal WT or *Siglec*^{-/-} mice were infected with GBS. Twenty-four hours later, total lung macrophages from infected (GBS; dashed lines) and control mice (Ctrl; administered sterile HBSS, solid lines) were analyzed by FACS, measuring sialoadhesin (left panels) and Siglec-E (right panels) expression. Isotype control plots for each Ab are shown in gray. Representative histogram plots from three independent experiments (**Continued**)

chromatin peaks in adult alveolar macrophages compared with neonatal cells (red boxes in Fig. 3D). Moreover, LPS exposure increased open chromatin in several regions around the *Siglec1* gene, suggesting that areas within the *Siglec1* gene might be less accessible in neonatal alveolar macrophages and that innate immune activation could activate changes in chromatin structure. Differentially accessible regions bound STAT6 in BMDMs but not STAT1. The promoter and upstream regions of *Siglec* contained more chromatin accessibility peaks in neonatal alveolar macrophages by ATAC-seq than in adult alveolar macrophages (Fig. 3E).

Expression of *Stat1* and *Stat6* mRNA was not statistically different between adult, juvenile (PND7), and neonatal (PND1) lung samples (Fig. 4A). To test if STAT6 was required for sialoadhesin expression, we measured sialoadhesin, Siglec-E, and Siglec-F expression in adult *Stat6*^{-/-} mice. Flow cytometry of alveolar macrophages from *Stat6*^{-/-} and WT adult mice did not detect differences in expression of the three cell surface macrophage Siglecs tested (Fig. 4B, 4C). Similarly, mRNA expression of *Siglec*, *Siglec1*, *Ifng*, and *Ifnb* was not statistically different between WT and *Stat6*^{-/-} lungs (Fig. 4D). These data suggested that STAT6 was not required for Siglec expression under basal conditions.

We next tested if deletion of the inhibitory Siglec-E would impact STAT1 expression in neonatal and adult lungs following GBS infection. In control lungs without GBS infection, STAT1 expression was observed in cells throughout the adult lung, including CD68⁺ macrophages (Fig. 5A). Following GBS infection, additional STAT1⁺ cells were visualized that expressed low levels of CD68 or were CD68⁻, suggesting recruitment of STAT1⁺ inflammatory cells (Fig. 5B). In contrast, lungs from adult *Siglec*^{-/-} mice showed a higher number of cells expressing STAT1 both in basal conditions and following GBS infection (Fig. 5D, 5E). Many of the STAT1⁺ cells in *Siglec*^{-/-} lungs after GBS infection exhibited low CD68 expression and had morphology consistent with monocytes (Fig. 5E). Measuring STAT1 fluorescence (normalized to the number of cells in each image) in Fig. 5C, 5F demonstrated the increased anti-STAT1 staining following GBS infection in both WT and *Siglec*^{-/-} lungs. In WT neonatal lungs, STAT1 expression was detected at low levels in multiple cell types (Fig. 5G). However, after GBS infection, the total anti-STAT1 staining decreased (Fig. 5H, 5I). In neonatal *Siglec*^{-/-} mice, GBS infection increased STAT1 expression, although perhaps to a lesser degree than observed in adult *Siglec*^{-/-} lungs (Fig. 5J–5L). These observations suggested that Siglec-E may play a role in inhibiting STAT1 expression in the mouse lung and that, in the presence of Siglec-E, GBS can suppress the immune response in neonates.

How these processes might also regulate sialoadhesin expression in the neonatal lung was not clear.

Modulation of sialoadhesin expression

To test how innate immune activation might regulate sialoadhesin expression, we incubated freshly isolated cells from PND2 lungs with individual innate immune activators or GM-CSF, known to promote alveolar macrophage maturation. Sialoadhesin expression was then measured in lung macrophages by flow cytometry. As shown in Fig. 6B, 38 h of culture with IFN γ , LPS, or GM-CSF each increased sialoadhesin expression. Because prenatal exposure to LPS leads to preterm delivery and developmental abnormalities in mice (24–26), we first tested if prenatal IFN could increase sialoadhesin expression in newborn mice. Timed pregnant mice were injected with either IFN α or IFN γ on embryonic day 18, two days prior to delivery (Fig. 6C). Both IFNs increased CD45⁺ leukocytes in PND0 mouse lungs (Fig. 6D). Although IFN γ increased the percentage of CD11b^{HI}/F4/80^{LO} cells (likely neutrophils), IFN α increased CD45⁺ cells lacking both CD11b and F4/80, consistent with lymphocytic influx. However, we did not detect increases in either sialoadhesin or Siglec-F in PND0 lung macrophage populations following IFN α or IFN γ exposure. Newborn mice exposed to prenatal IFN α or IFN γ also died soon after delivery, preventing measurement of macrophage maturation or sialoadhesin expression at later time points.

GM-CSF-stimulated alveolar macrophage differentiation requires peroxisome proliferator-activated receptor γ (PPAR γ) (27). To test the ability of PPAR γ activation to promote sialoadhesin expression at birth, we administered the PPAR γ agonist rosiglitazone to embryonic day 18 pregnant mice. Prenatal rosiglitazone treatment increased the percentage of lung macrophages expressing both F4/80 and CD11b (Fig. 7A). Although rosiglitazone increased Siglec-F expression in PND0 (newborn) macrophages as measured by flow cytometry, we did not detect increased sialoadhesin expression (Fig. 7B). When measured at PND4, rosiglitazone reduced the number of lung macrophages lacking either sialoadhesin or Siglec-F expression (Fig. 7C), suggesting that although PPAR γ activation drives postnatal alveolar macrophage maturation, prenatal rosiglitazone treatment was not sufficient to significantly increase sialoadhesin expression in newborn lung macrophages, when it might provide protection against GBS acquired at birth.

DISCUSSION

Understanding how the newborn lung immune system detects and responds to GBS is paramount to developing better therapies and preventative approaches. In most cases, GBS infection

are shown. (B and C) *Siglec1* (left panels) and *Siglec* (right panels) mRNA expression in neonatal (B) or adult (C) mice infected with either WT or Δ neuA GBS measured by real-time PCR. Data are represented as fold change compared with uninfected control animals using *Gapdh* for normalization. Samples were obtained and analyzed 0.5, 6, and 24 h following infection. (D) *I11b* mRNA expression in neonatal (left panel) and adult (right panel) C57BL/6 mice infected with either WT or Δ neuA GBS. Lung samples were obtained and analyzed 0.5, 6, and 24 h following infection. *I11b* expression was measured by real-time PCR. * $p < 0.05$ using unpaired two-tailed t test in comparing samples indicated by horizontal bars.

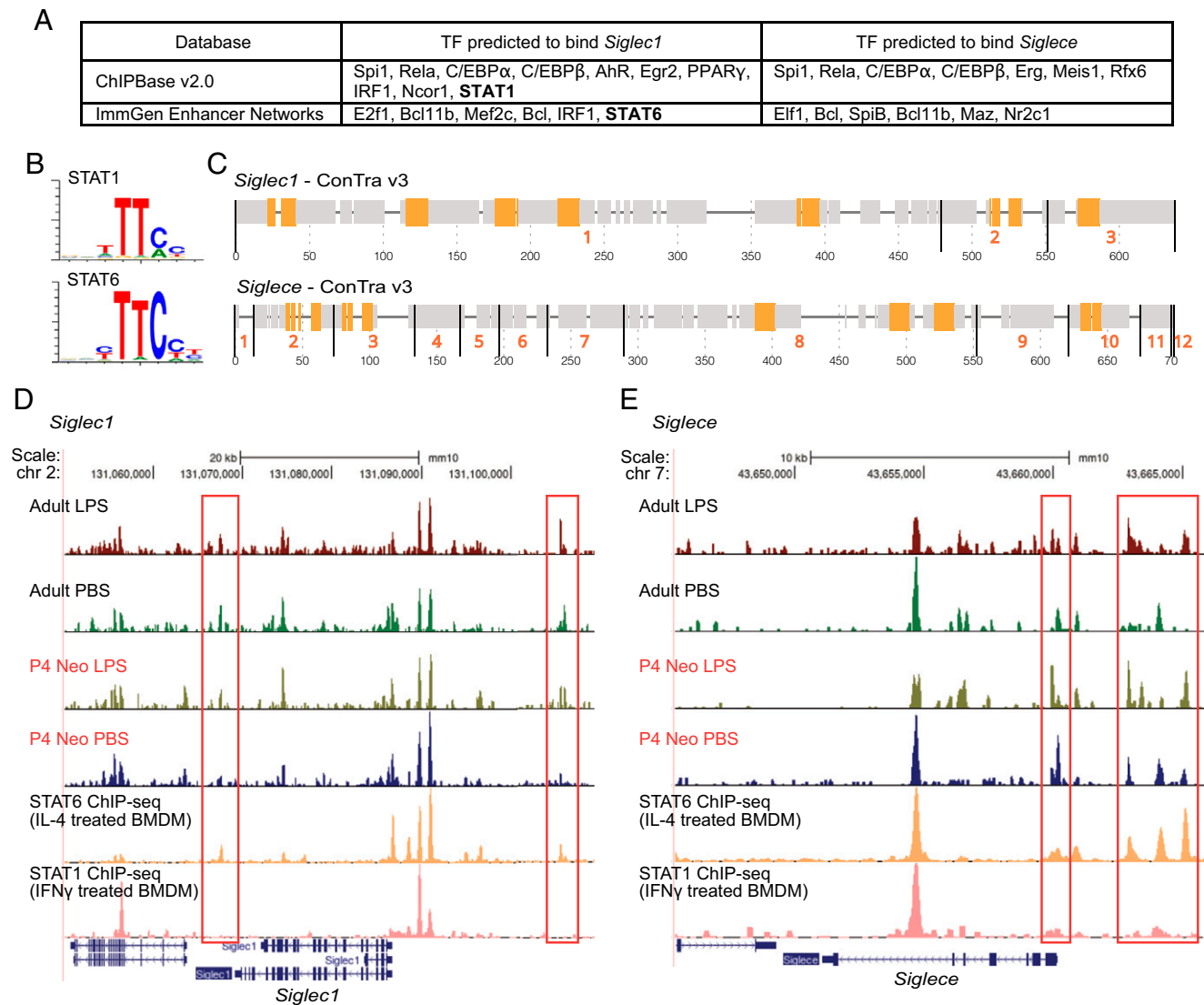


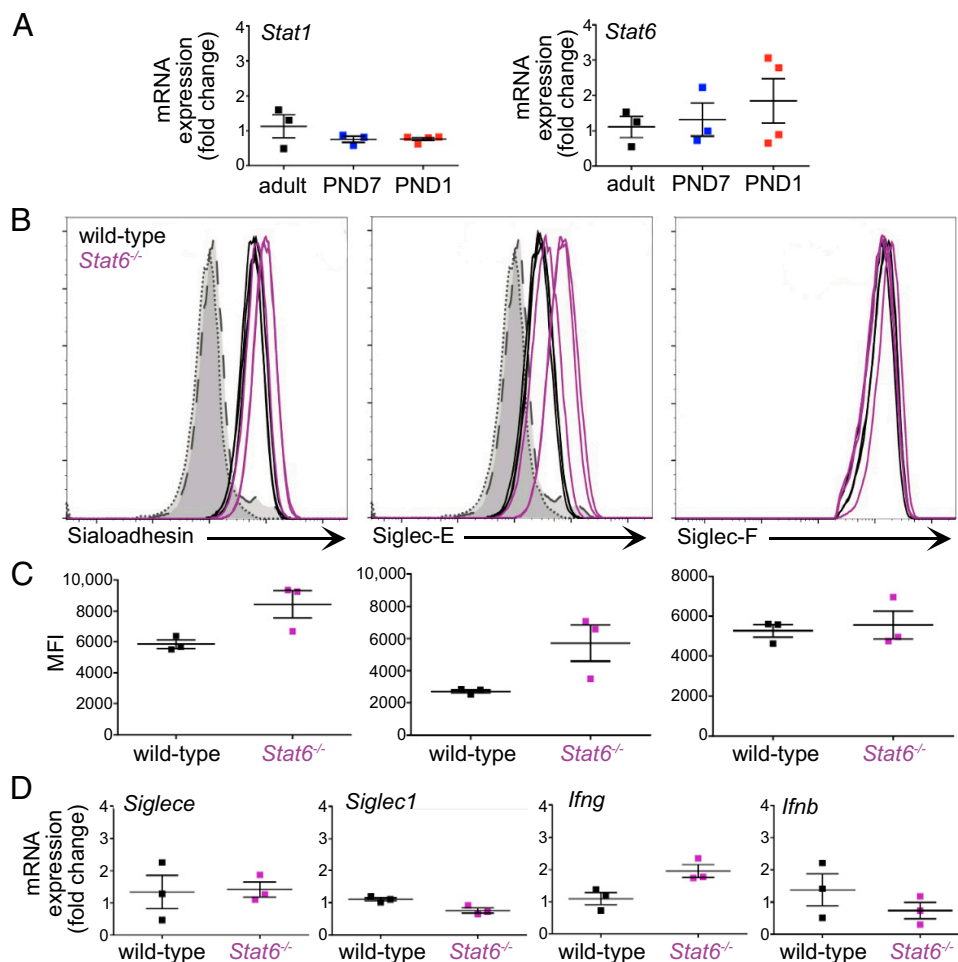
FIGURE 3. Predicted STAT binding within murine *Siglec1* and *Siglece* promoters. (A) Table showing the top results of transcription factors (TFs) predicted to bind the promoter regions of *Siglec1* and *Siglece* from the ChIPBase version 2.0 and ImmGen Enhancer Networks databases. (B) Comparison of the similar sequences predicted to bind STAT1 and STAT6 from JASPAR CORE. (C) Predicted STAT6 binding sites in the murine *Siglec1* and *Siglece* promoter regions (ConTra version 3). Conserved sequence regions are identified within black lines and labeled with orange numerals. Predicted STAT6 binding sequences identified with orange bars. (D and E). ATAC-seq and ChIP-seq data (15–17) showing open chromatin and STAT binding in alveolar macrophages (ATAC-seq) and BMDMs (ChIP-seq). For the ATAC-seq datasets, alveolar macrophages were isolated from adult and PND4 C57BL/6 mice administered either intranasal PBS or LPS (0.1 μ g/g body weight) 2 h prior to isolation and cell sorting. ChIP-seq data were obtained from mouse BMDMs treated with either IL-4 (STAT6) or IFN γ (STAT1) for 1 h prior to fixation. Peaks were aligned within the UCSC Genome Browser. OCRs and STAT binding peaks are shown for *Siglec1* (D) and *Siglece* (E).

occurs when newborns aspirate bacteria during passage through the birth canal. The neonatal window of susceptibility to GBS pneumonia appears to close rapidly, because older infants and children rarely develop GBS lung infections. Building on previous research demonstrating the developmental deficiency of sialoadhesin expression in newborn alveolar macrophages, we show here that GBS infection in vivo suppresses sialoadhesin expression in vivo via interactions between the

sialylated bacterial capsule and the inhibitory receptor Siglec-E. Interestingly, GBS suppression of *Siglec1* transcript levels (encoding sialoadhesin) by GBS occurred in both neonates and adults. Presumably, the higher basal sialoadhesin expression in adult macrophages prior to infection ensures adequate protection compared with the lower levels observed in neonatal cells. Alternatively, adult lungs may possess additional host protection mechanisms not available to neonates. Additional

FIGURE 4. STAT6 was not required for Siglec expression.

(A) *Stat1* (left) and *Stat6* (right) mRNA expression in adult (black squares, $n = 3$), PND7 (blue squares, $n = 3$), and PND1 (red squares, $n = 4$) lungs measured by real-time PCR and represented as fold change compared with WT using *Gapdh* for normalization. (B and C) Flow cytometric analysis of sialoadhesin, Siglec-E, and Siglec-F cell surface expression in WT (black) and *Stat6*^{-/-} adult alveolar macrophages. FACS histograms shown in (B), MFI plotted in (C). $n = 3$ for each genotype. (D) *Siglece*, *Siglec1*, *Ifng*, and *Ifnb* mRNA expression measured in adult WT and *Stat6*^{-/-} lungs by real-time PCR and represented as fold change compared with WT using *Gapdh* for normalization. $n = 3$ for each genotype.



experiments could test how dynamic expression of Siglecs following infection contribute to lung immunity in adults. Inhibition of *Siglec1* expression was also transient in both neonates and adults, suggesting a dynamic and evolving interaction between pathogen and host.

Increasing sialoadhesin expression in newborn macrophages could protect neonates against GBS infection. Sialoadhesin is considered a downstream marker of chronic inflammation and IFN activation in both experimental models and human immune cells (8, 28–32). Although in vitro treatments with GM-CSF, LPS, and IFN γ were each successful in increasing sialoadhesin expression in cultured neonatal mouse lung macrophages, we were not able to replicate these increases in vivo. Not only did prenatal injection of either IFN α or IFN γ fail to increase sialoadhesin expression in P0 macrophages, but the resulting inflammation led to neonatal death. More targeted activation of the IFN signaling pathway, or its downstream mediators, may be required in immature alveolar macrophages to achieve successful upregulation of sialoadhesin at birth.

The fetal and neonatal lung microenvironment may actively suppress sialoadhesin expression until the postnatal period, making it challenging to induce upregulation at birth. Our examination of ATAC-seq and ChIP-seq data identified reduced

accessibility of several regions of the *Siglec1* gene in neonatal alveolar macrophages, suggesting potential epigenetic silencing of *Siglec1* transcription during the perinatal period (15–17). The *Siglec1* promoter regions contain multiple predicted STAT binding sites, but our experiments to test how STAT family members might affect sialoadhesin expression did not yield clear insights. Siglec expression in lung macrophages was not significantly different in *Stat6*^{-/-} mice. Additionally, although *Siglece*^{-/-} knockout adult mice had large increases in STAT1-expressing cells with GBS infection, neonatal *Siglece*^{-/-} lungs did not show the same dramatic impact of *Siglece* deletion on STAT1 expression, before or after infection. Therefore, our explorations aimed at regulating sialoadhesin expression around the time of birth require further efforts.

The postnatal upregulation of sialoadhesin expression could be part of the alveolar macrophage differentiation program that occurs in mice within 3–4 d after birth (7, 33). GM-CSF and downstream activation of PPAR γ are both required for normal alveolar macrophage differentiation, making them potential candidates for increasing sialoadhesin expression (7, 33, 34). However, fetal lung macrophages are also exposed to GM-CSF (33), and our experiments activating PPAR γ with prenatal rosiglitazone failed to increase sialoadhesin expression.

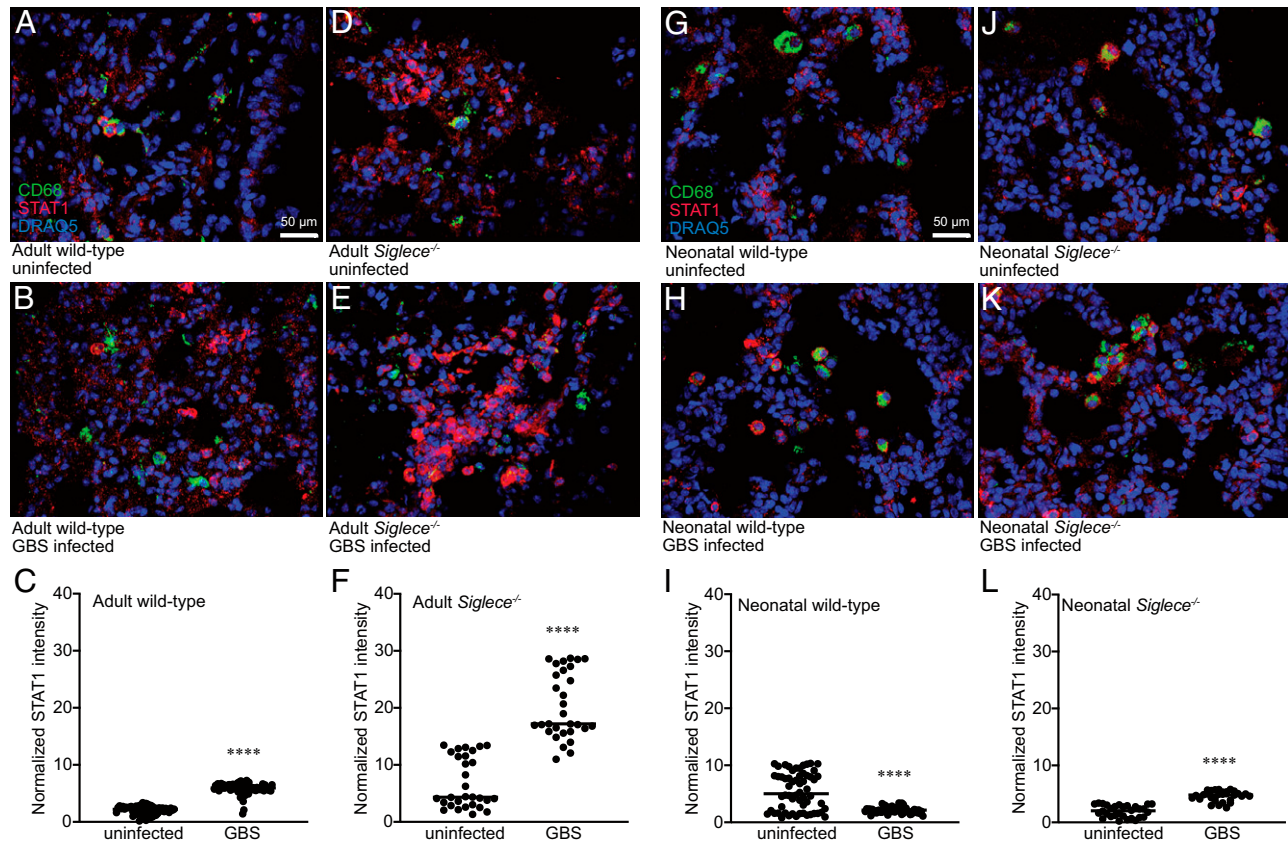


FIGURE 5. STAT1 expression in WT and *Siglec*^{-/-} lungs following GBS infection.

Lungs from adult (A–F) and neonatal (G–L) mice were fixed, sectioned, and immunostained for the macrophage marker CD68 (green) and STAT1 (red). DRAQ5 was used as a nuclear stain and shown in blue. All samples were obtained 24 h postinfection with GBS (B, E, H and K) or sterile saline (A, D, G and J). STAT1 expression was quantified by measuring total anti-STAT1 fluorescence intensity and normalizing to the DRAQ5 nuclear stain fluorescence intensity in each image for normalization (C, F, I and L). (A–C) Adult WT (C57BL/6) mice. (D–F) Adult *Siglec*^{-/-} mice. (G–I) Neonatal (PND0) WT (C57BL/6) mice. (J–L) Neonatal *Siglec*^{-/-} mice. Optical sections were acquired by laser scanning confocal microscopy using a 40 \times objective, and three-dimensional merged images are shown. Each image is representative of multiple images obtained in three independent experiments. **** $p < 0.0001$, $n = 30$ –75 images for each condition.

Glycan–Siglec interactions regulate both macrophage differentiation and immune tolerance during pregnancy (35, 36). For example, increased levels of α 2,3- and α 2,6-sialic acid appear in the circulation of pregnant women, only to fall to previous levels after delivery (37). At the fetal–maternal interface, the binding of the secreted glycoprotein glycodefin-A to Siglec-7 promotes monocyte differentiation into decidual macrophages with an immune tolerant phenotype (38). Although much of the recent research on glycan–receptor interactions during fetal immune development has focused on the placental microenvironment (39, 40), similar principles of regulating immune suppression of immunity until after delivery may also apply to fetal lung macrophage development, promoting the expression of Siglec-E but not sialoadhesin.

GBS appears to take advantage of glycan-driven promotion of immune tolerance. Host glycans with terminal sialic acid modifications can bind to Siglec receptors containing intracellular inhibitory motifs, leading to recruitment of SHP phosphatases and the inhibition of innate immune signaling (41–43). In at least

several GBS serotypes, the Sia α 2,3Gal β 1,4GlcNAc structure within the capsular polysaccharide is identical to the terminal sialic acid structures found in host glycans, enabling them to bind inhibitory Siglec receptors and prevent immune detection and inflammation (8, 11, 44). GBS binding to human Siglec-9 (homolog of mouse Siglec-E) on neutrophils and platelets inhibits cellular antibacterial responses (10, 11). The poly- α 2,8-Sia capsules of *Escherichia coli* K1 and *Neisseria meningitidis* serotype B bind Siglec-11 in the CNS in an analogous manner, limiting neural inflammation and immune response (45–47). By binding to these inhibitory Siglec receptors, these bacteria inhibit immune signaling and suppress the inflammatory response, avoiding detection and facilitating colonization and invasive infection.

To counteract immune evasion, host sialoadhesin can bind to the identical sialic acid motifs present in the GBS capsule as does Siglec-E (and Siglec-9), but instead stimulates inflammation, bacterial phagocytosis, and killing (8, 48). Our data showed that GBS can inhibit expression of sialoadhesin in vivo through Siglec-E engagement. Although the impact appears

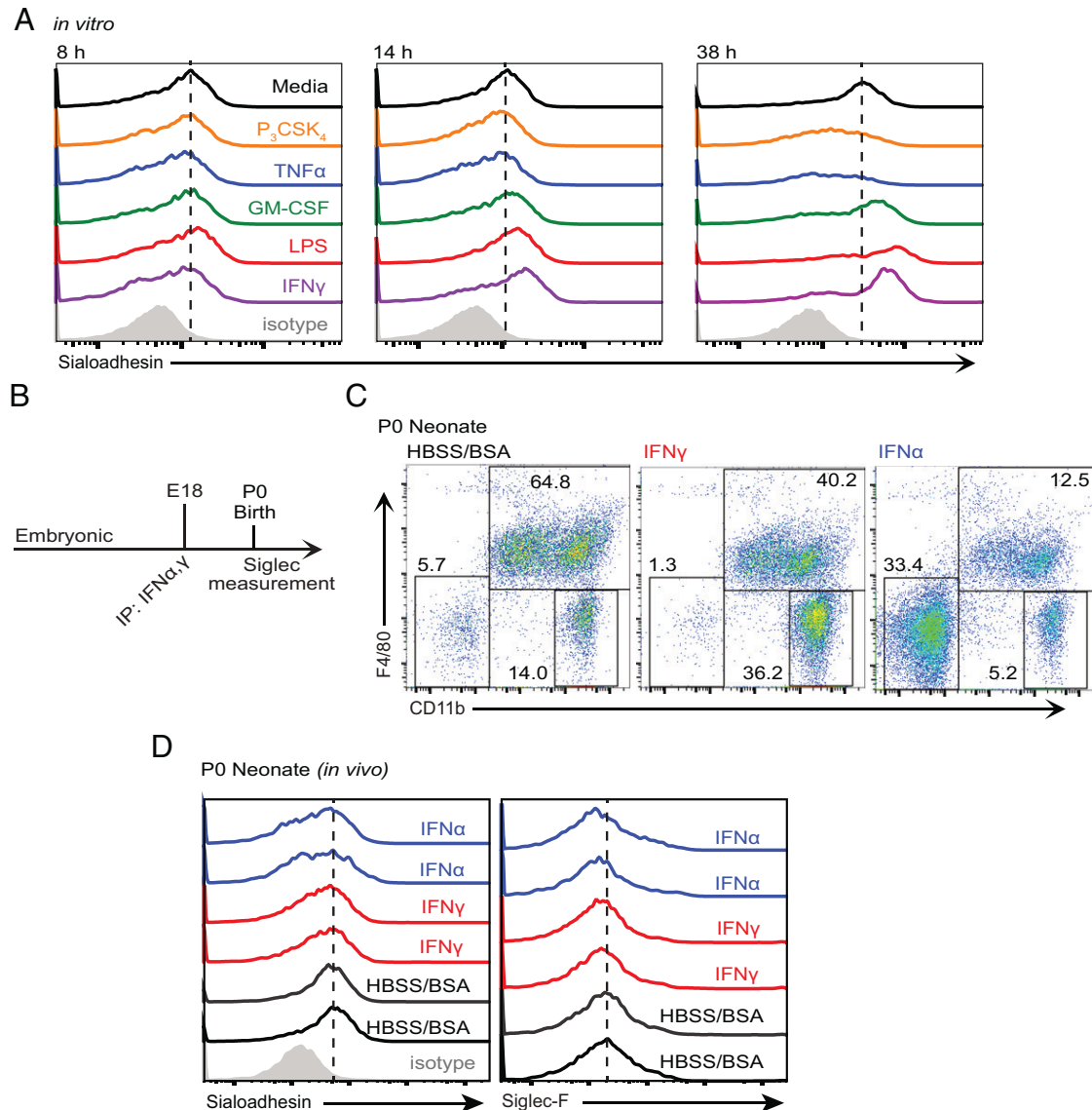


FIGURE 6. Regulation of sialoadhesin expression by inflammatory mediators.

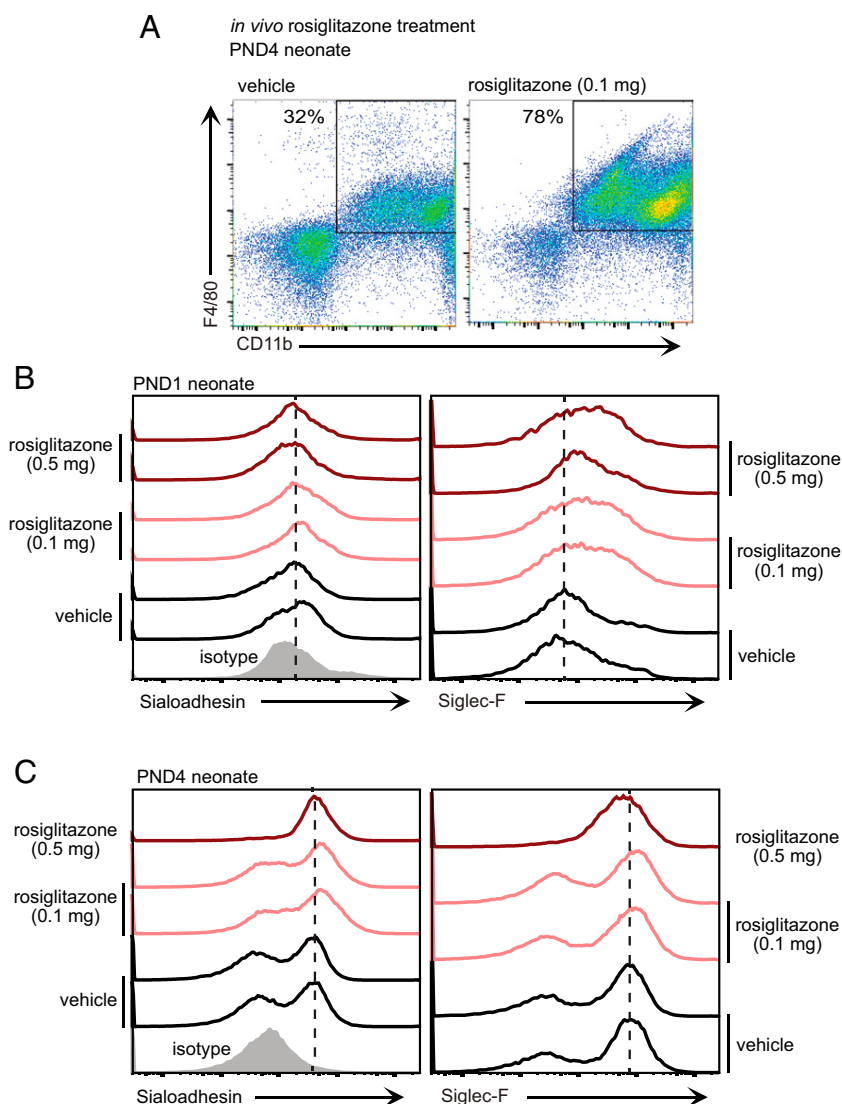
(A) Total cell suspensions from PND2 C57BL/6 lungs were cultured for 8 h, 14 h, or 38 h in the presence of Pam₃CSK₄ (300 ng/ml), TNF α (10 ng/ml), GM-CSF (10 ng/ml), LPS (250 ng/ml), or IFN γ (10 ng/ml). Sialoadhesin expression was measured in CD45⁺/F4/80⁺/CD11b⁺ macrophages by FACS, and histogram data are shown. Dashed line represents peak sialoadhesin expression frequency in control samples for comparison across treatments. Histogram for isotype control shown in gray. Representative histograms from three independent experiments are shown. (B) Diagram of the timeline used for *in vivo* experiments. Timed pregnant C57BL/6 mice were injected with i.p. IFN α or IFN γ (dosage) or HBSS (control) on embryonic day 18. Following delivery, lung immune cell populations and sialoadhesin expression were measured by flow cytometry. (C) IFN α increased the percentage of CD45⁺/CD11b^{HI}/F4/80[−] neutrophils, whereas IFN γ increased the percentage of CD45⁺/CD11b[−]/F4/80[−] cells, likely representing lymphocytes. Representative data from three independent experiments are shown. (D) Prenatal IFN injection did not increase sialoadhesin or Siglec-F expression as measured by FACS in PND0 CD45⁺/F4/80⁺/CD11b⁺ lung macrophages. Histograms from two of three independent experiments are shown.

transient, slowing the upregulation of sialoadhesin expression in newborns even for just a few hours could allow devastating bacterial spread, pneumonia, and sepsis. Delaying maturation of innate immunity against GBS may be even more impactful in the preterm infants who have a higher incidence rate of GBS sepsis than term infants (1). Importantly, newborn mouse lungs are in the saccular stage of development and similar to 30–32-wk

gestation humans. Future studies examining developmental maturation of Siglec expression may need to include additional postnatal time points in mice and correlation with human samples when available. The back-and-forth interactions between the GBS capsule and host pattern recognition receptors illustrate the molecular mimicry used by GBS to avoid detection. Although the potential causal role of sialoadhesin in autoimmune

FIGURE 7. Prenatal administration of rosiglitazone was not able to increase neonatal macrophage sialoadhesin expression.

(A) Lung macrophages from PND4 mice exposed to vehicle control or 0.1 mg rosiglitazone were analyzed by FACS. Rosiglitazone increased the percentage of F4/80^{hi} macrophages, consistent with stimulation of macrophage differentiation. Data shown are representative of three independent experiments. (B) Expression of sialoadhesin and Siglec-F in CD45⁺/F4/80⁺/CD11b⁺ lung macrophages obtained from PND1 neonatal mice exposed on embryonic day 18 to vehicle control or rosiglitazone (either 0.1 mg or 0.5 mg) was measured by FACS. Each histogram represents an independent experiment out of three separate replicates. Background staining using an isotype control Ab shown in gray. Dashed line represents peak intensity in vehicle control samples. (C) Expression of sialoadhesin and Siglec-F in CD45⁺/F4/80⁺/CD11b⁺ lung macrophages obtained from PND4 neonatal mice exposed to vehicle control or rosiglitazone (either 0.1 mg or 0.5 mg on E18) was measured by FACS. Each histogram represents an independent experiment out of three separate replicates. Background staining using an isotype control Ab shown in gray. Dashed line represents peak intensity in vehicle control samples.



and autoinflammatory diseases is not fully understood, the observed increase in sialoadhesin-positive immune cells in multiple chronic inflammatory disease states (21, 49, 50) raises questions about potential consequences detrimental to the host resulting from our ever-evolving battle against microbial pathogens.

DISCLOSURES

The authors have no financial conflicts of interest.

ACKNOWLEDGMENTS

We thank Drs. Harold Hoffman, Lori Broderick, Mamata Sivagnanam, and Ajit Varki and the members of the Prince and Nizet laboratories for their helpful comments and insight.

REFERENCES

1. Nanduri, S. A., S. Petit, C. Smelser, M. Apostol, N. B. Alden, L. H. Harrison, R. Lynfield, P. S. Vagnone, K. Burzlaff, N. L. Spina, et al. 2019.

- Epidemiology of invasive early-onset and late-onset group B streptococcal disease in the United States, 2006 to 2015: multistate laboratory and population-based surveillance. *JAMA Pediatr.* 173: 224–233.
2. Armistead, B., E. Oler, K. Adams Waldorf, and L. Rajagopal. 2019. The double life of group B streptococcus: asymptomatic colonizer and potent pathogen. *J. Mol. Biol.* 431: 2914–2931.
3. Francois Watkins, L. K., L. McGee, S. J. Schrag, B. Beall, J. H. Jain, T. Pondo, M. M. Farley, L. H. Harrison, S. M. Zansky, J. Baumbach, et al. 2019. Epidemiology of invasive group B streptococcal infections among nonpregnant adults in the United States, 2008–2016. *JAMA Intern. Med.* 179: 479–488.
4. Invernizzi, R., C. M. Lloyd, and P. L. Molyneaux. 2020. Respiratory microbiome and epithelial interactions shape immunity in the lungs. *Immunology* 160: 171–182.
5. Joshi, N., J. M. Walter, and A. V. Misharin. 2018. Alveolar macrophages. *Cell. Immunol.* 330: 86–90.
6. Crocker, P. R., J. C. Paulson, and A. Varki. 2007. Siglecs and their roles in the immune system. *Nat. Rev. Immunol.* 7: 255–266.
7. Williams, M., I. De Kleer, S. Henri, S. Post, L. Vanhoutte, S. De Prijck, K. Deswarte, B. Malissen, H. Hammad, and B. N. Lambrecht. 2013. Alveolar macrophages develop from fetal monocytes that

- differentiate into long-lived cells in the first week of life via GM-CSF. *J. Exp. Med.* 210: 1977–1992.
8. Chang, Y. C., J. Olson, A. Louie, P. R. Crocker, A. Varki, and V. Nizet. 2014. Role of macrophage sialoadhesin in host defense against the sialylated pathogen group B *Streptococcus*. *J. Mol. Med. (Berl.)* 92: 951–959.
9. McMillan, S. J., R. S. Sharma, E. J. McKenzie, H. E. Richards, J. Zhang, A. Prescott, and P. R. Crocker. 2013. Siglec-E is a negative regulator of acute pulmonary neutrophil inflammation and suppresses CD11b beta2-integrin-dependent signaling. *Blood* 121: 2084–2094.
10. Carlin, A. F., S. Uchiyama, Y. C. Chang, A. L. Lewis, V. Nizet, and A. Varki. 2009. Molecular mimicry of host sialylated glycans allows a bacterial pathogen to engage neutrophil Siglec-9 and dampen the innate immune response. *Blood* 113: 3333–3336.
11. Uchiyama, S., J. Sun, K. Fukahori, N. Ando, M. Wu, F. Schwarz, S. S. Siddiqui, A. Varki, J. D. Marth, and V. Nizet. 2019. Dual actions of group B *Streptococcus* capsular sialic acid provide resistance to platelet-mediated antimicrobial killing. *Proc. Natl. Acad. Sci. U. S. A.* 116: 7465–7470.
12. Lund, S. J., K. A. Patras, J. M. Kimmey, A. Yamamura, L. D. Butcher, P. G. B. Del Rosario, G. E. Hernandez, A. M. McCoy, O. Lakhdari, V. Nizet, and L. S. Prince. 2020. Developmental immaturity of Siglec receptor expression on neonatal alveolar macrophages predisposes to severe group B streptococcal infection. *iScience* 23: 101207.
13. Lewis, A. L., H. Cao, S. K. Patel, S. Diaz, W. Ryan, A. F. Carlin, V. Thon, W. G. Lewis, A. Varki, X. Chen, and V. Nizet. 2007. NeuA sialic acid O-acetyltransferase activity modulates O-acetylation of capsular polysaccharide in group B *Streptococcus*. *J. Biol. Chem.* 282: 27562–27571.
14. Weiman, S., S. Daresh, A. F. Carlin, A. Varki, V. Nizet, and A. L. Lewis. 2009. Genetic and biochemical modulation of sialic acid O-acetylation on group B *Streptococcus*: phenotypic and functional impact. *Glycobiology* 19: 1204–1213.
15. Honda, A., M. A. Hoeksema, M. Sakai, S. J. Lund, O. Lakhdari, L. D. Butcher, T. C. Rambaldo, N. M. Sekiya, C. A. Nasamran, K. M. Fisch, et al. 2022. The lung microenvironment instructs gene transcription in neonatal and adult alveolar macrophages. *J. Immunol.* 208: 1947–1959.
16. Hoeksema, M. A., Z. Shen, I. R. Holtman, A. Zheng, N. J. Spann, I. Cobo, M. Gymrek, and C. K. Glass. 2021. Mechanisms underlying divergent responses of genetically distinct macrophages to IL-4. *Sci. Adv.* 7: eabf9808.
17. Ostuni, R., V. Piccolo, I. Barozzi, S. Polletti, A. Termanini, S. Bonifacio, A. Curina, E. Prosperini, S. Ghisletti, and G. Natoli. 2013. Latent enhancers activated by stimulation in differentiated cells. *Cell* 152: 157–171.
18. Zhou, K. R., S. Liu, W. J. Sun, L. L. Zheng, H. Zhou, J. H. Yang, and L. H. Qu. 2017. ChIPBase v2.0: decoding transcriptional regulatory networks of non-coding RNAs and protein-coding genes from ChIP-seq data. *Nucleic Acids Res.* 45: D43–D50.
19. Kreft, L., A. Soete, P. Hulpiau, A. Botzki, Y. Saeys, and P. De Bleser. 2017. ConTra v3: a tool to identify transcription factor binding sites across species, update 2017. *Nucleic Acids Res.* 45: W490–W494.
20. Rempel, H., C. Calosing, B. Sun, and L. Pulliam. 2008. Sialoadhesin expressed on IFN-induced monocytes binds HIV-1 and enhances infectivity. *PLoS One* 3: e1967.
21. Fercoq, F., E. Remion, S. J. Frohberger, N. Vallarino-Lhermitte, A. Hoerauf, J. Le Quesne, F. Landmann, M. P. Hubner, L. M. Carlin, and C. Martin. 2019. IL-4 receptor dependent expansion of lung CD169⁺ macrophages in microfilaria-driven inflammation. *PLoS Negl. Trop. Dis.* 13: e0007691.
22. Van Bockstal, L., D. Bulte, M. Van den Kerkhof, L. Dirx, D. Mabile, S. Hendrickx, P. Delpitte, L. Maes, and G. Caljon. 2020. Interferon alpha favors macrophage infection by visceral *Leishmania* species through upregulation of sialoadhesin expression. *Front. Immunol.* 11: 1113.
23. Heng, T. S., and M. W. Painter. Immunological Genome Project Consortium. 2008. The Immunological Genome Project: networks of gene expression in immune cells. *Nat. Immunol.* 9: 1091–1094.
24. Romero, R., M. Mazor, and B. Tartakovsky. 1991. Systemic administration of interleukin-1 induces preterm parturition in mice. *Am. J. Obstet. Gynecol.* 165: 969–971.
25. O’Loughlin, E., J. M. P. Pakan, D. Yilmazer-Hanke, and K. W. McDermott. 2017. Acute in utero exposure to lipopolysaccharide induces inflammation in the pre- and postnatal brain and alters the glial cytoarchitecture in the developing amygdala. *J. Neuroinflammation* 14: 212.
26. Prince, L. S., H. I. Dieperink, V. O. Okoh, G. A. Fierro-Perez, and R. L. Lallone. 2005. Toll-like receptor signaling inhibits structural development of the distal fetal mouse lung. *Dev. Dyn.* 233: 553–561.
27. Schneider, C., S. P. Nobs, M. Kurrer, H. Rehrauer, C. Thiele, and M. Kopf. 2014. Induction of the nuclear receptor PPAR-gamma by the cytokine GM-CSF is critical for the differentiation of fetal monocytes into alveolar macrophages. *Nat. Immunol.* 15: 1026–1037.
28. Bao, G., Z. Han, Z. Yan, Q. Wang, Y. Zhou, D. Yao, M. Gu, B. Chen, S. Chen, A. Deng, and R. Zhong. 2010. Increased Siglec-1 expression in monocytes of patients with primary biliary cirrhosis. *Immunol. Invest.* 39: 645–660.
29. Biesen, R., C. Demir, F. Barkhudarova, J. R. Grun, M. Steinbrich-Zollner, M. Backhaus, T. Haupl, M. Rudwaleit, G. Riemekasten, A. Radbruch, et al. 2008. Sialic acid-binding Ig-like lectin 1 expression in inflammatory and resident monocytes is a potential biomarker for monitoring disease activity and success of therapy in systemic lupus erythematosus. *Arthritis Rheum.* 58: 1136–1145.
30. van der Kuyl, A. C., R. van den Burg, F. Zorgdrager, F. Groot, B. Berkhout, and M. Cornelissen. 2007. Sialoadhesin (CD169) expression in CD14⁺ cells is upregulated early after HIV-1 infection and increases during disease progression. *PLoS One* 2: e257.
31. Xiong, Y. S., Y. H. Zhou, G. H. Rong, W. L. Wu, Y. Liang, Z. X. Yang, H. L. Geng, and R. Q. Zhong. 2009. Siglec-1 on monocytes is a potential risk marker for monitoring disease severity in coronary artery disease. *Clin. Biochem.* 42: 1057–1063.
32. York, M. R., T. Nagai, A. J. Mangini, R. Lemaire, J. M. van Seventer, and R. Lafyatis. 2007. A macrophage marker, Siglec-1, is increased on circulating monocytes in patients with systemic sclerosis and induced by type I interferons and toll-like receptor agonists. *Arthritis Rheum.* 56: 1010–1020.
33. Gschwend, J., S. P. M. Sherman, F. Ridder, X. Feng, H. E. Liang, R. M. Locksley, B. Becher, and C. Schneider. 2021. Alveolar macrophages rely on GM-CSF from alveolar epithelial type 2 cells before and after birth. *J. Exp. Med.* 218: e20210745.
34. Dorr, D., B. Obermayer, J. M. Weiner, K. Zimmermann, C. Anania, L. K. Wagner, E. M. Lyras, V. Sapozhnikova, D. Lara-Astiaso, F. Prosper, et al. 2022. C/EBPbeta regulates lipid metabolism and Pparg isoform 2 expression in alveolar macrophages. *Sci. Immunol.* 7: eabj0140.
35. Clark, G. F. 2014. The role of glycans in immune evasion: the human foetoembryonic defence system hypothesis revisited. *Mol. Hum. Reprod.* 20: 185–199.
36. Lubbers, J., E. Rodriguez, and Y. van Kooyk. 2018. Modulation of immune tolerance via Siglec-sialic acid interactions. *Front. Immunol.* 9: 2807.
37. Jansen, B. C., A. Bondt, K. R. Reiding, E. Lonardi, C. J. de Jong, D. Falck, G. S. Kammeijer, R. J. Dolhain, Y. Rombouts, and M. Wuhler. 2016. Pregnancy-associated serum N-glycome changes studied by high-throughput MALDI-TOF-MS. *Sci. Rep.* 6: 23296.
38. Vijayan, M., C. L. Lee, V. H. H. Wong, X. Wang, K. Bai, J. Wu, H. Koistinen, M. Seppala, K. F. Lee, W. S. B. Yeung, et al. 2020. Decidual glycodefin-A polarizes human monocytes into a decidual macrophage-like phenotype through Siglec-7. *J. Cell Sci.* 133: jcs244400.
39. Lam, K. K., P. C. Chiu, C. L. Lee, R. T. Pang, C. O. Leung, H. Koistinen, M. Seppala, P. C. Ho, and W. S. Yeung. 2011. Glycodefin-A protein

- interacts with Siglec-6 protein to suppress trophoblast invasiveness by down-regulating extracellular signal-regulated kinase (ERK)/c-Jun signaling pathway. *J. Biol. Chem.* 286: 37118–37127.
40. Sammar, M., M. Siwetz, H. Meiri, V. Fleming, P. Altevogt, and B. Huppertz. 2017. Expression of CD24 and Siglec-10 in first trimester placenta: implications for immune tolerance at the fetal-maternal interface. *Histochem. Cell Biol.* 147: 565–574.
 41. Stefanski, A. L., M. D. Renecke, A. Kramer, S. Sehgal, P. Narasimhan, K. K. Rumer, and V. D. Winn. 2022. Siglec-6 signaling uses Src kinase tyrosine phosphorylation and SHP-2 recruitment. *Cells* 11: 3427.
 42. Walter, R. B., B. W. Raden, R. Zeng, P. Hausermann, I. D. Bernstein, and J. A. Cooper. 2008. ITIM-dependent endocytosis of CD33-related Siglecs: role of intracellular domain, tyrosine phosphorylation, and the tyrosine phosphatases, Shp1 and Shp2. *J. Leukoc. Biol.* 83: 200–211.
 43. Ulyanova, T., D. D. Shah, and M. L. Thomas. 2001. Molecular cloning of MIS, a myeloid inhibitory Siglec, that binds protein-tyrosine phosphatases SHP-1 and SHP-2. *J. Biol. Chem.* 276: 14451–14458.
 44. Chang, Y. C., J. Olson, F. C. Beasley, C. Tung, J. Zhang, P. R. Crocker, A. Varki, and V. Nizet. 2014. Group B *Streptococcus* engages an inhibitory Siglec through sialic acid mimicry to blunt innate immune and inflammatory responses in vivo. *PLoS Pathog.* 10: e1003846.
 45. Yang, J., W. Ma, Y. Wu, H. Zhou, S. Song, Y. Cao, C. Wang, X. Liu, J. Ren, J. Duan, et al. 2021. O-acetylation of capsular polysialic acid enables *Escherichia coli* K1 escaping from Siglec-mediated innate immunity and lysosomal degradation of *E. coli*-containing vacuoles in macrophage-like cells. *Microbiol. Spectr.* 9: e0039921.
 46. Schwarz, F., C. S. Landig, S. Siddiqui, I. Secundino, J. Olson, N. Varki, V. Nizet, and A. Varki. 2017. Paired Siglec receptors generate opposite inflammatory responses to a human-specific pathogen. *EMBO J.* 36: 751–760.
 47. Landig, C. S., A. Hazel, B. P. Kellman, J. J. Fong, F. Schwarz, S. Agarwal, N. Varki, P. Massari, N. E. Lewis, S. Ram, and A. Varki. 2019. Evolution of the exclusively human pathogen *Neisseria gonorrhoeae*: human-specific engagement of immunoregulatory Siglecs. *Evol. Appl.* 12: 337–349.
 48. Chang, Y. C., and V. Nizet. 2014. The interplay between Siglecs and sialylated pathogens. *Glycobiology* 24: 818–825.
 49. Kikuchi, K., M. Iida, N. Ikeda, S. Moriyama, M. Hamada, S. Takahashi, H. Kitamura, T. Watanabe, Y. Hasegawa, K. Hase, et al. 2018. Macrophages switch their phenotype by regulating Maf expression during different phases of inflammation. *J. Immunol.* 201: 635–651.
 50. Li, G., R. Yamasaki, M. Fang, K. Masaki, H. Ochi, T. Matsushita, and J. I. Kira. 2018. Novel disease-modifying anti-rheumatic drug iguratimod suppresses chronic experimental autoimmune encephalomyelitis by down-regulating activation of macrophages/microglia through an NF-kappaB pathway. *Sci. Rep.* 8: 1933.